A rotation around the z-axis generates the effect visible in Figure 33; the most noticeable feature is the lateral displacement of the focal spot by the correct amount (and because the MM is a double XOU, the outer XOU focus is displaced more due to the larger radius of curvature, so the spot is split into two), plus some focus broadening.

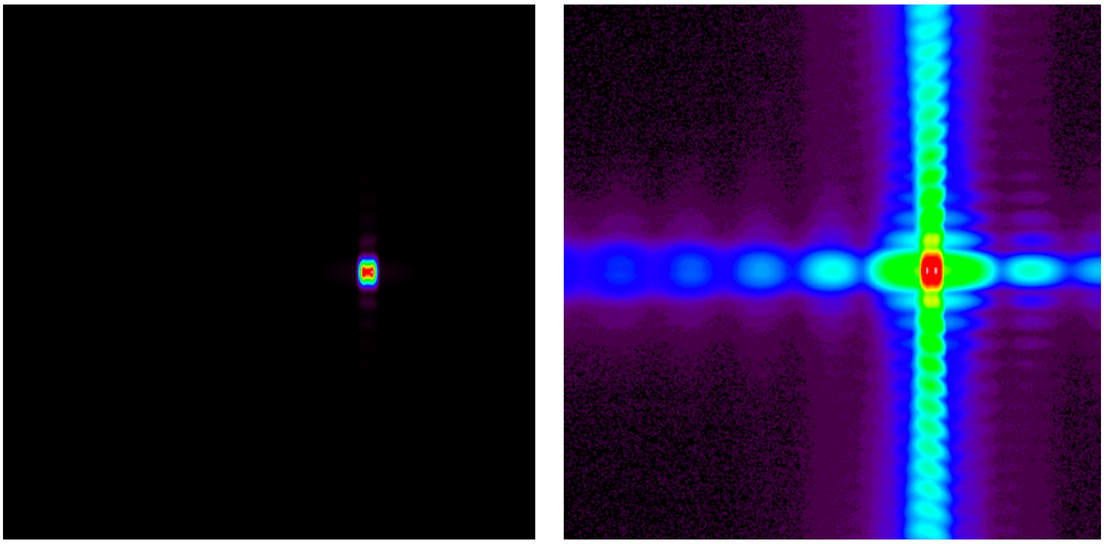

Figure 33: simulation at λ = 40 Å, 2 mm field, of the MM with the primary stack misaligned with respect to the secondary one. Rotation around the z-axis by 100 arcsec. (left) Linear color scale, (right) log color scale. The centroid is displaced by 0.362 mm (= 100 arcsec $\times$ 753 mm radius). The focus centering option was not selected.

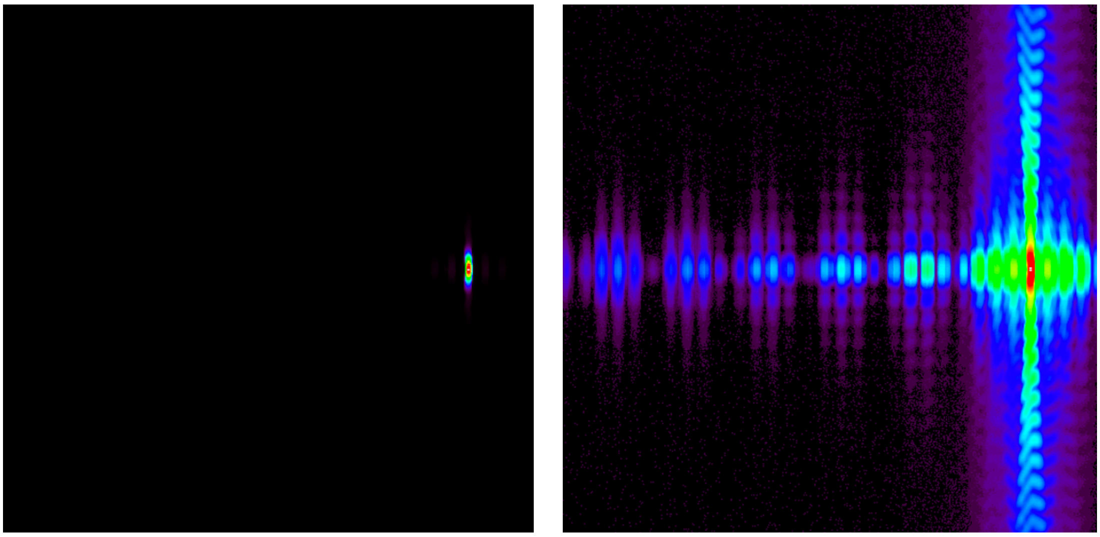

Figure 34: simulation at λ = 40 Å, 2 mm field, of the MM with the primary stack misaligned with respect to the secondary one. Translation along the x-axis by +0.75 mm. (left) Lin color scale, (right) log color scale. The centroid is displaced by 0.74 mm.

The effect of translating the primary stack is trickier. In general, the mismatch between the rib position reduces the collecting area considerably. Moreover, a translation along the x-axis of the primary stack causes a noticeable aberration and a displacement of the spot approximately by the same amount of the stack translation (Figure 34).

The focal spot is even more sensitive to translations along the y-axis (Figure 35), as it directly affects the slope change along the optics meridian. Due to the resulting mismatch between primary and secondary pores, even a small misalignment causes a relevant aberration. The "triplication" of the spot occurs because the displacement is, in this example, approximately half the pore height; therefore, half of the pore areas are still aligned with their respective ones in the secondary stack. This generates the central focus. The upper and the lower spots, resulting from the pore areas that are in correspondence with the "wrong ones" of the secondary stack, tend to disappear when the misalignment in y is a multiple of the pore height.

Finally, translations along the z-axis (Figure 36) mostly cause a spot defocusing, even if the primary stack needs to be considerably taken apart from the hyperbolic one for some aberration to be seen. The translation also entails vertical displacement of the beam.

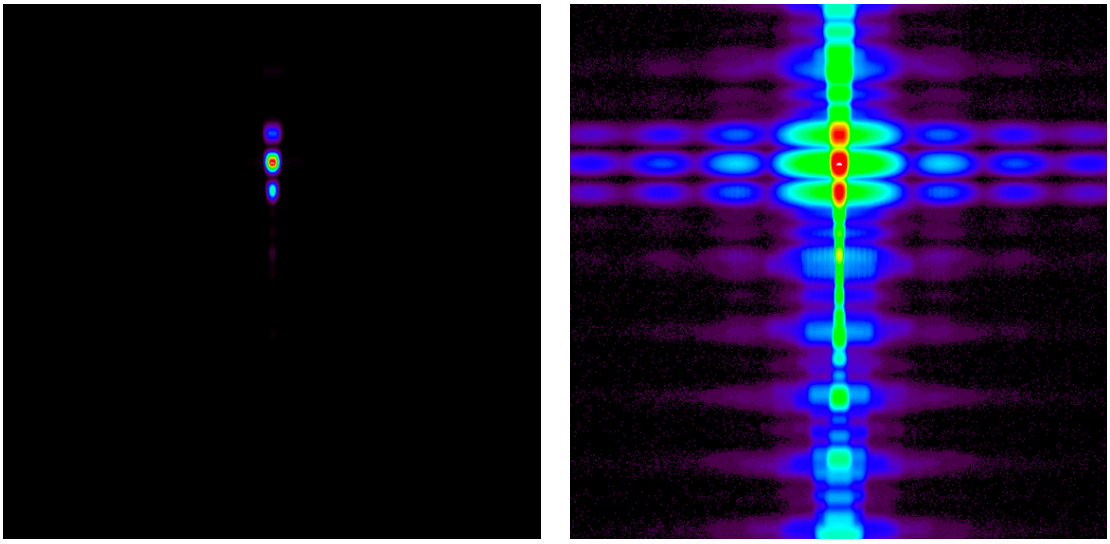

Figure 35: simulation at λ = 40 Å, 2 mm field, of the MM with the primary stack misaligned with respect to the secondary one. Translation along the y-axis by 0.4 mm. (left) Lin color scale, (right) log color scale.

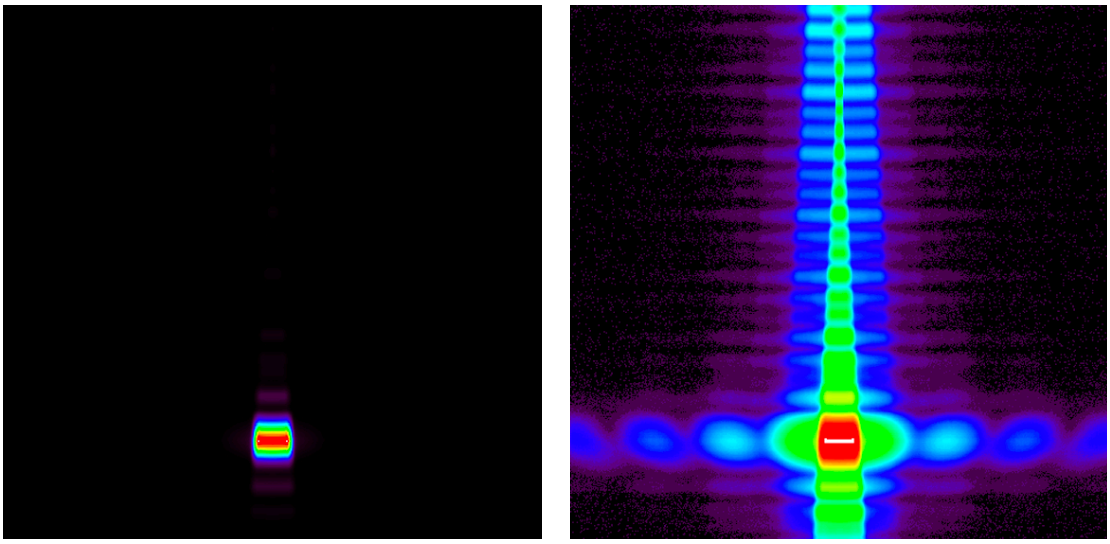

Figure 36: simulation at λ = 40 Å, 2 mm field, of the MM with the primary stack misaligned with respect to the secondary one. Translation along the z-axis by 20 mm, toward the source. (left) Linear color scale, (right) log color scale.

3.4. Sagittal errors

We now consider the case of sinusoidal errors along the plate width (Sect. 2.2.2, case 2a). Superimposing a single harmonic along the arc of the plates degrades the sagittal focusing as modeled in Figure 37. As expected, if the perturbation is exactly co-sinusoidal, then the diffraction figure exhibits sharp maxima near the edges (Figure 37, left), where the perturbation is locally flat. If the plate width includes a few periods of the harmonic, additional fringes can appear in between (Figure 37, right).

Another option in the current version of SWORDS is the randomization of the amplitudes and the phases according to a quasi-gaussian distribution. This has the effect shown in Figure 38, with a change in the intensity distribution throughout the arc. Another kind of imperfection consists in curvature radius errors in the azimuthal (sagittal) direction (Sect. 2.2.2, case 2b). The expected effect is the focal spot broadening along the plate width (Figure 39, left). If the curvature radius is increased, the azimuthal focal length is increased in proportion, and so the resulting arc is bent downwards, just like the mirror module. The focal spot can be subsequently re-focused by shifting the focal plane, at the expense of the tangential focusing and the convergence of the plate pairs. This is shown in Figure 39, right. Finally, edge effects can be modeled as explained in Sect. 2.2.2, case 2c; two examples are displayed in Figure 40.

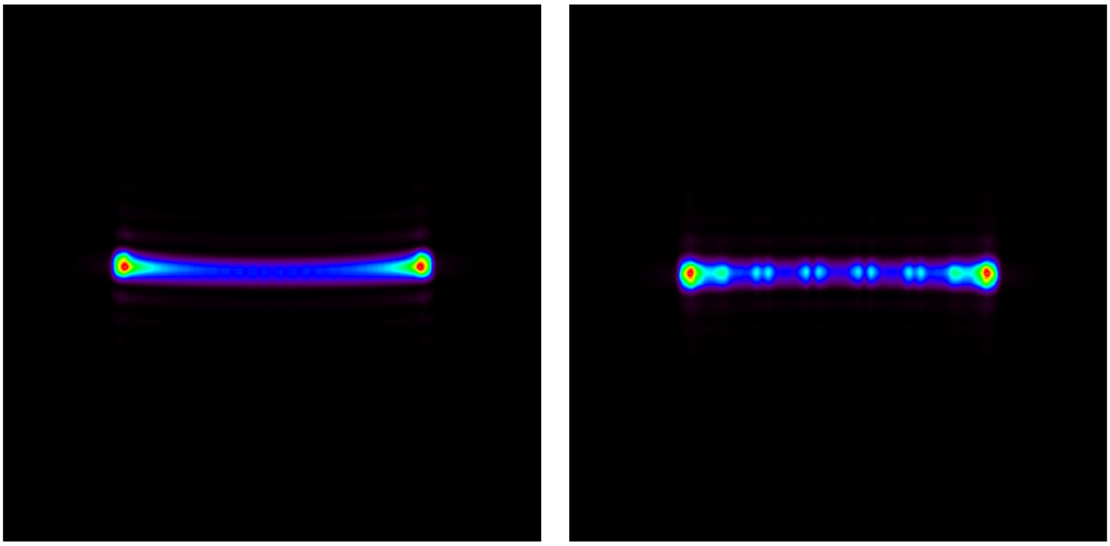

Figure 37: simulation at λ = 40 Å, 2 mm field, of the MM with a sagittal error in each plate, with constant phase and amplitudes. Linear color scale. (left) period equal to twice the plate width and 20 μm amplitude, (right) period equal to ½ the plate width and 5 μm amplitude.

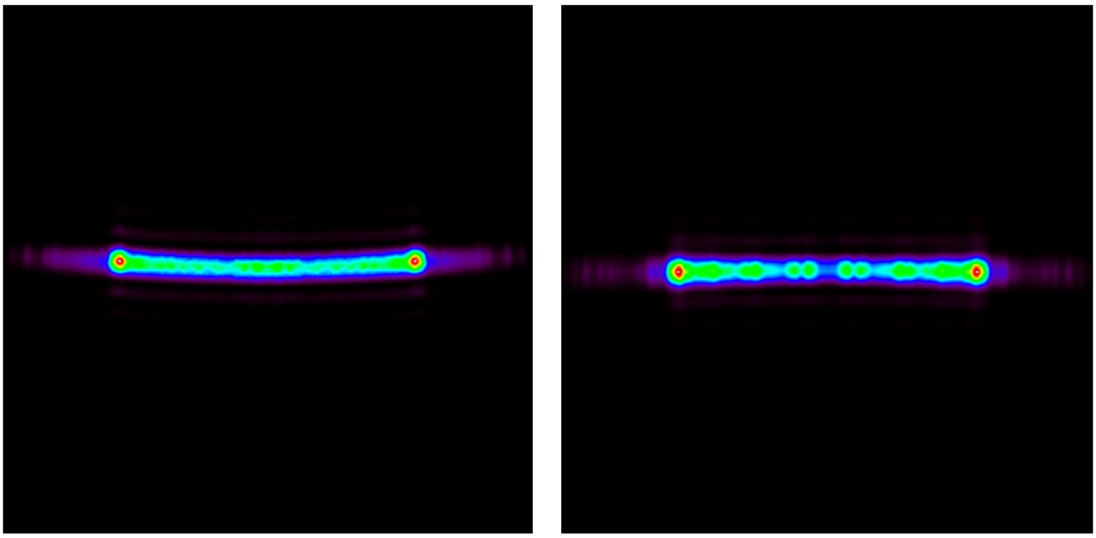

Figure 38: just like Figure 37, but this time the amplitudes are randomized through the stack (rms = ¼ of the amplitude).

DOI: 10.13140/RG.2.2.22411.36647

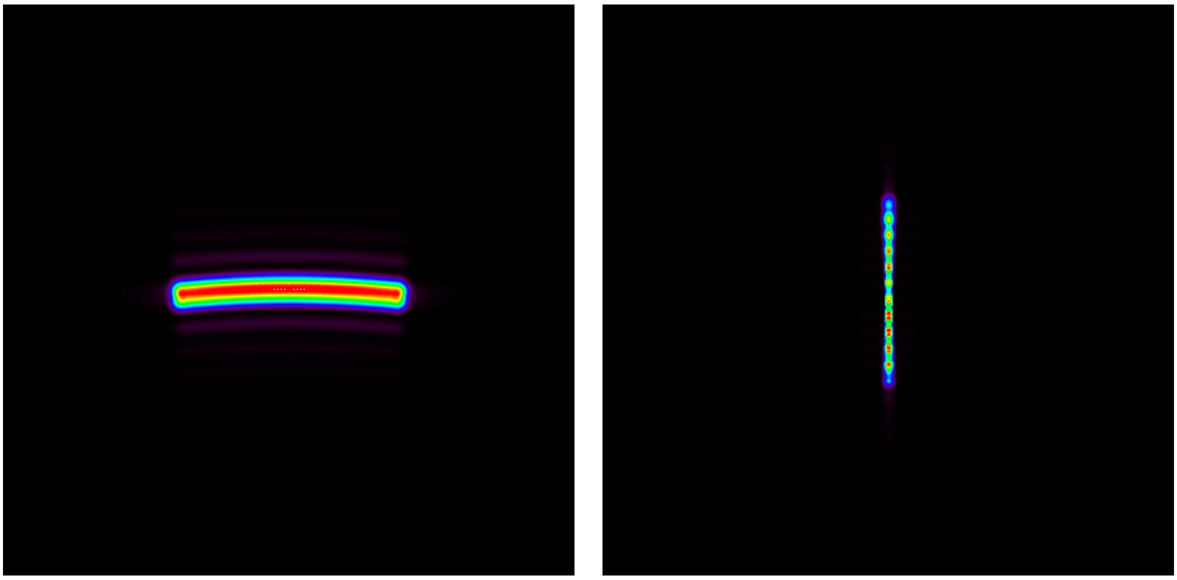

Figure 39: simulation at λ = 40 Å, 2 mm field, of the MM with the same curvature radius error on the primary and the secondary stack. Linear color scale. (left) a +7.5 mm curvature radius error, in the nominal focus. (right) Focal plane re-focused, placed at 7.5/753×12000 mm = 119 mm beyond the nominal focus.

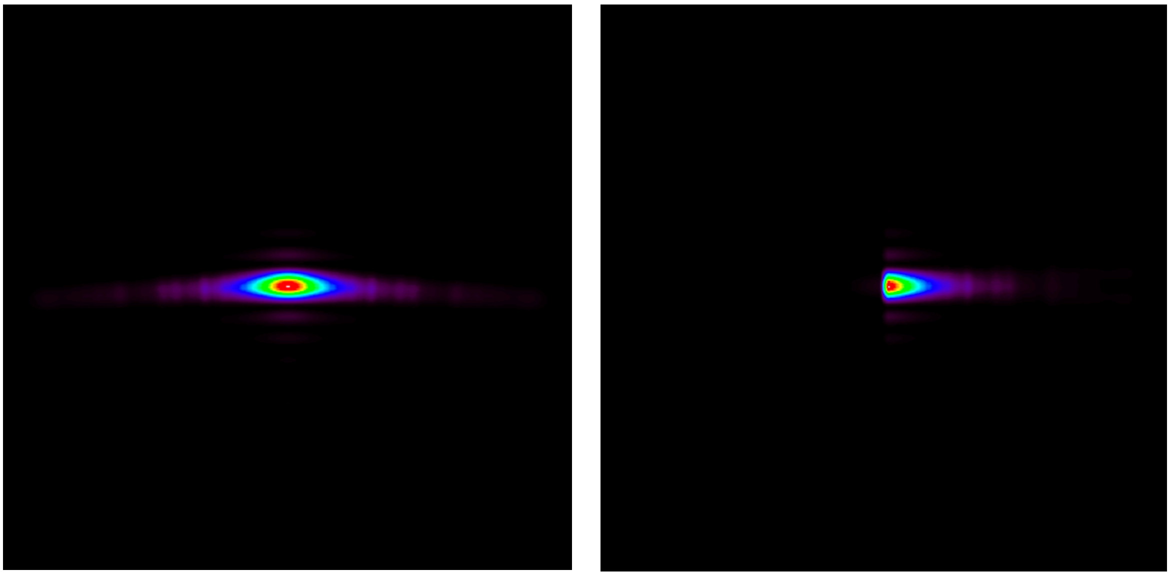

Figure 40: simulation at λ = 40 Å, 2 mm field, of the MM with sagittal edge effects in order to return a Lorentzian profile in the sagittal direction, 30 µm PtV. Linear color scale. (left) even profile. (right) odd profile.

3.5. Tangential errors

Different kinds of tangential errors can be simulated, as mentioned in Sect. 2.2.2, case 3. In reality, the simplest possible profile error was introduced in Sect. 2.2.1 as a double cone geometry. The departure from the perfect Wolter-I shape entails imperfect tangential focusing, with details slightly depending on the wedge configuration. The effect is shown in Figure 41, along with some de-centering due to the tangency of the double cone to the Wolter profile occurring at the IP. Therefore, the rays reflected near the IP end at the detector center, but the remainder of the focused wavefront is deflected at positive *y*.

Other analytical errors that can be set by the user include sinusoidal errors of variable period and amplitude (Sect. 2.2.2, case 3a) and edge effect of fixed amplitude with even and odd parity (Sect. 2.2.2 case 3b). Some diffraction figures are displayed in Figure 42 and Figure 43, also randomizing the sinusoidal phases and amplitudes selecting the appropriate options. The user can combine different defect and inspect the effect on the diffracted figure. All the simulations can be repeated at any light wavelengths.

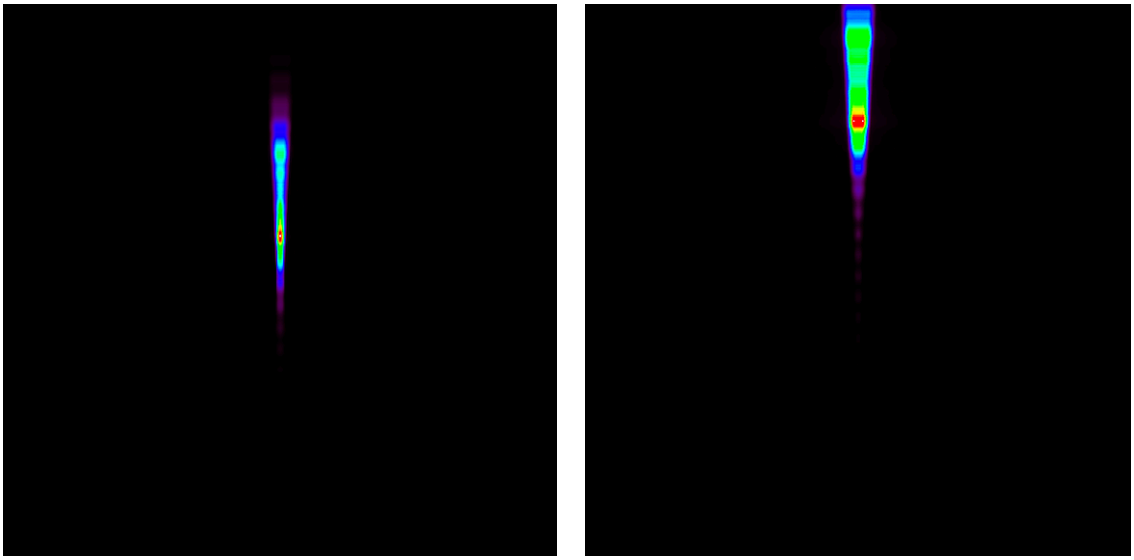

Figure 41: simulation at λ = 40 Å, 2 mm field, for stacked plates with a double cone profile. Linear color scale. (left) single XOU, (right) full MM.

Figure 42: simulation at λ = 40 Å, 2 mm field, of the MM with a sinusoidal error along the plate length having (left) a period L and a constant 0.2 µm amplitude on the primary stack. This multiple peak pattern corresponds to that of a sinusoidal grating with this period and amplitude. (right) the same, with randomized amplitudes, averages out the position of the peaks, so returning a much smoother PSF.

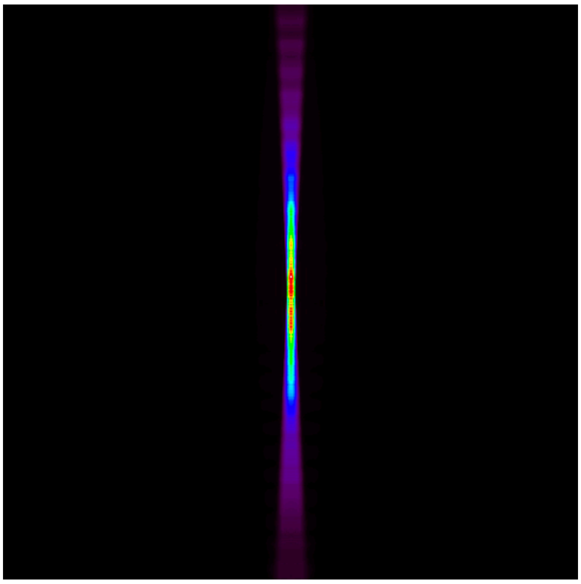

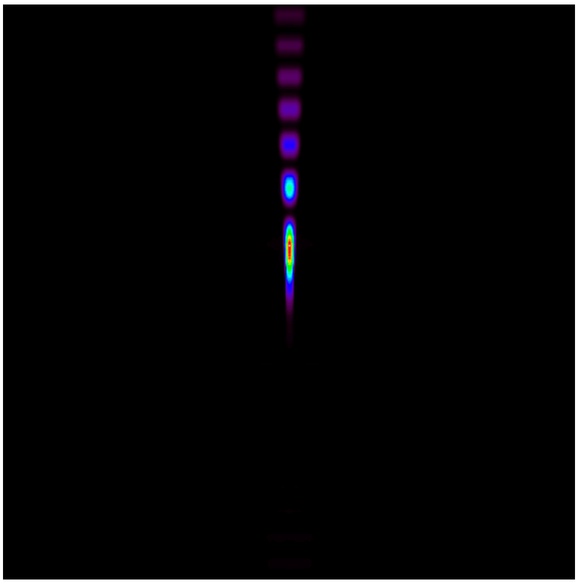

Figure 43: simulation at λ = 40 Å, 2 mm field, of the MM with a 1 µm edge effect along the plate length (left) even profile, (right) odd profile. Linear color scale.

3.6. Polynomial errors

A polynomial function can be defined (Sect. 2.2.2, case 4) as profile error, the same for all the plates in the stack, on the primary mirror stack only, even though in this release it is easy for the user to impart a polynomial deformation to both plates. In this example, the coefficients used for the simulation are x_1y_1 = 1e-4, x_2y_1 = 1e-5, x_1y_2 = -3e-4, x_2y_2 = 4e-5, x_3y_0 = 4e-4, in the respective proper units to return a map in microns. The result of the computation is shown in Figure 44, along with a detail of the CPF showing the deformation of each plate.

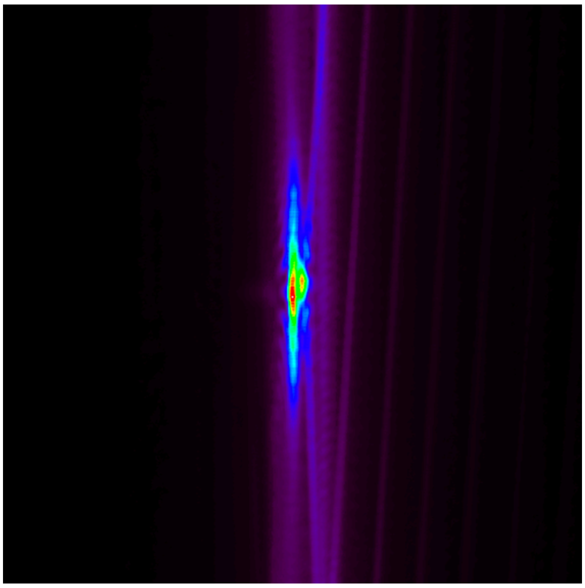

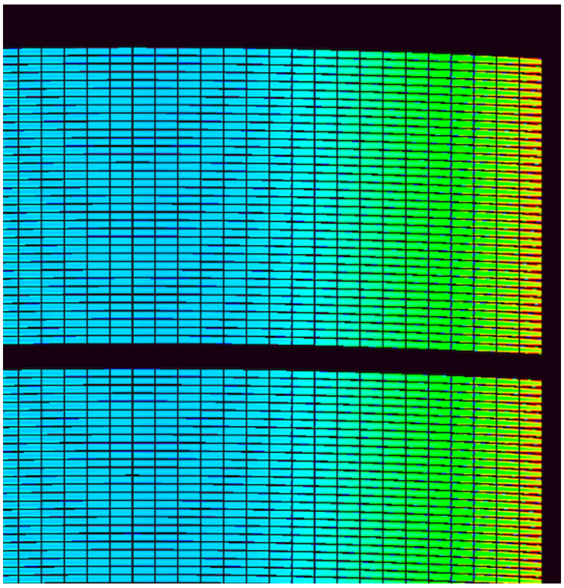

Figure 44: (left) simulation at λ = 40 Å, 2 mm field, of the MM with a 2D polynomial error with coefficients specified by the user. Linear color scale. (right) detail of the CPF showing the polynomial deformation.

3.7. Tabulated errors

As anticipated in Sect. 2.2.3, the user can also upload a set of measured maps of figure errors and fit it to the plate area (in this example, only the plates of the primary stack with the same file for all the plates). When the maps are loaded, they are resampled, projected onto the aperture of each plate, and included in the CPF (Figure 14). Processing the CPF returns, as expected, a broadening of the focal spot, mostly in the incidence plane, as shown in the example of Figure 45.

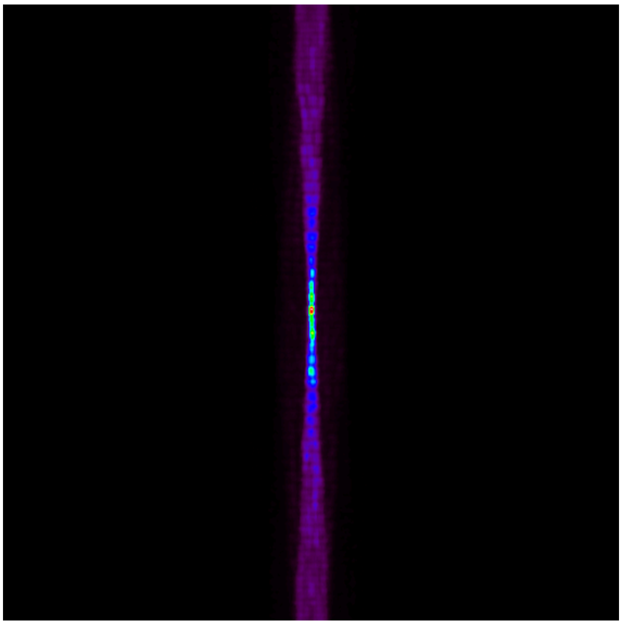

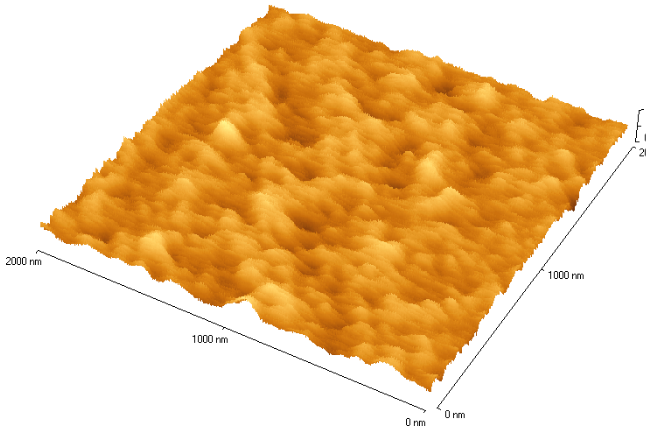

Figure 45: (left) simulation at λ = 40 Å, 3 mm field, of the MM with the tabulated error shown in Figure 14. Linear color scale. (right) the profile error map used for the simulation. The vertical scale is always assumed in microns. The lateral size is not relevant, as the map is stretched in order to fit the plate dimensions.

4. Final remarks

This user manual has provided some instructions for easy usage of the SWORDS 3.7.2 simulation program for SPO mirror modules. More functionalities, such as the extension to groups of MMs and to the full MM assembly of ATHENA, will be implemented in the next releases. Users are cordially invited to report program bugs and suggestions to daniele.spiga@inaf.it.